Evaluation of Different Satellite Images for Urban Land Use Analysis: A case study of Greater Manchester, United Kingdom.

ABSTRACT

Background: The complexity of an urban area makes mapping it very difficult as its surface materials are highly spatial and spectrally diverse. This study evaluates the problems associated with remote sensing of urban land cover types.

Methodology: Three satellite image sensors; Disaster Monitoring Constellation (DMC), Landsat TM and colour infrared were used to investigate their potentials in mapping and characterizing land cover in a part of Greater Manchester. Supervised and unsupervised image classifications were used to map urban land use and cover.

Results: The satellite image sensors and their accuracy were statistically tested to see if there is a significant relationship between them. The colour infrared image was the best in discriminating among different types of land cover with an overall accuracy of 80% followed by the Landsat image with an overall accuracy of 61% while the DMC image had the least potential in discriminating among different types of land cover with an overall accuracy of 55%.

Conclusion: The colour infrared image is the most suitable for urban land cover analysis as the misclassifications are minimal compared to the other two and the features can be vividly recognized due to its spatial resolution.

Keywords: Urban land use mapping, satellite images, spatial resolution, spectral resolution, accuracy assessment.

INTRODUCTION

Remote sensing has the considerable potential to produce thematic maps that represent spatially continuous and highly consistent spatial and temporal scales of the earth`s surface Z[1,2]. Remotely sensed data are usually deployed for image classification which can subsequently be used to describe the land cover of a region [3]. Although, remotely sensed images have been successfully used in mapping a wide range of land covers at varying spatial and temporal scales, their full potential as a land cover information source is yet to be realized [4][5].

Urban environment has been regarded as one of the most challenging areas in remote sensing. This is due to the high spatial and spectral diversity of surface materials, making the urban environment highly heterogeneous. Urban surface types usually create spectral diversity that greatly exceeds the natural environment. Over time, studies have reported problems arising from

remote sensing of urban areas [6,7] with some suggesting a rule of thumb of 5m spatial resolution for mapping urban areas [8,9].

Despite the developments of satellite imaging technology, land use and land cover maps, and image processing statistics remain a challenge [10,11]. Very few studies have compared the accuracy of different image classification methods using different images obtained using different satellite sensors [12–14]. Researchers have attempted to improve resolution and precision, leading to more noticeable change detection [6,15]. However, with improved models, misclassification is still a challenge [16], and differentiation between land use types remains challenging [17]. This research compares the result of supervised and unsupervised image classifications of three different satellite sensors acquired at approximately the same time to assess their efficacy in discriminating urban land cover types and their accuracy level assessed. It also examines the effect of the satellite image sensor`s spatial resolution on the accuracy assessment.

MATERIALS AND METHODS

Study Site

The study site is in the mid-east of Greater Manchester Metropolitan County in North West England. It is a heavily urbanized county made up of several settlements and vast built-up areas (figure 2). It runs through two Greater Manchester metropolitan counties, covering some of North-East Manchester and the eastern part of Salford (figure 1).

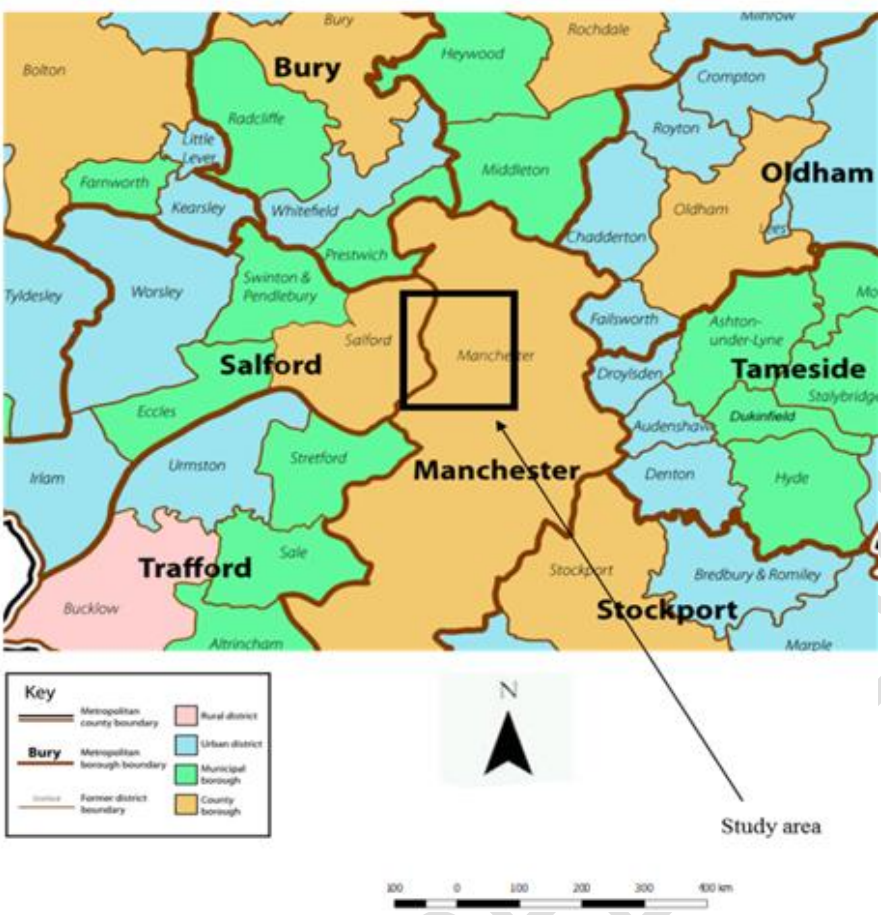

Source: http://www.greatermanchestersurveyors.co.uk/

Figure 1: Map of the study area; the center of the town of Greater Manchester

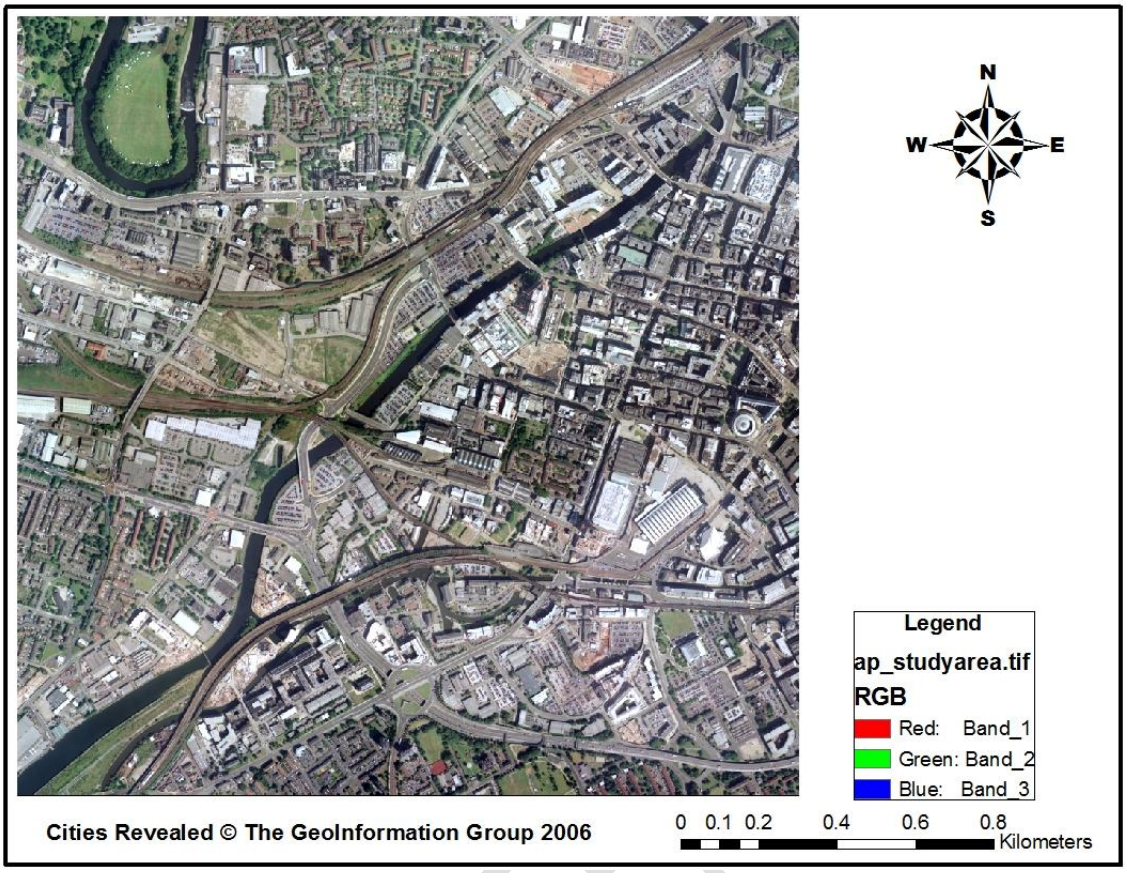

Figure 2: Aerial Photograph of the study area, the town center of Greater Manchester

The study site comprises different buildings, a river, vegetation types, parks, and a good rail and road network (figure 2). It has a wide range of land cover types like that of Anderson [18] and is therefore appropriate for urban area study and will be appropriate for assessing the efficacy of different images in discriminating among various types of land cover, including vegetation types, water bodies, and buildings by different sensors.

Data Collection

The data sets used for this project are Landsat a 4-5 TM image from the United States Geological Survey Agency (USGS) EarthExplorer database http://edcsns17.cr.usgs.gov/NewEarthExplorer/. The image was acquired on the 10th of June 2006. It has seven bands with only three bands of the sensors assigned to the three primary colours to make it a false colour composite [19]. The near infrared band displayed through a red filter, the red band through a green filter and the green band through a blue filter. Each band has a spatial resolution of 30m with band 6 originally 120m but resampled to 30m. The image was downloaded as level 1 geotiff file.

The second is Disaster Monitoring Constellation (DMC) image from DMC International Imaging http://www.dmcii.com/ The image was acquired by Nigeriasat DMC satellite on the 10th of May

2006. It is also a false colour composite and was downloaded as an ortholevel tiff image. It has a spatial resolution of 32m.

The third is a colour infrared image from Bluesky http://www.bluesky-world.com/. The image was acquired on the 22nd of June 2010. It has three bands and is a false colour composite with a spatial resolution of 0.5m and was downloaded as level tiff file.

For complete and accurate characterization of ground features from remotely sensed data, Steven [20,21] states that ground data is required. Because of the high resolution orthorectified images of modern aerial photographs can be used as additional complementary data to other geo-referenced data or as a standalone base map. Several researchers have used aerial photographs as reference data [22–24]. They are highly valued because they are the only materials with high credibility on terrain coverage and use [25]. The reference data used for this research is an aerial photograph of the study area acquired on the 20th of December 2006 by The GeoInformation Group http://www.geoinformationgroup.co.uk and has a spatial resolution of 0.125m.

Preprocessing Methods

The images were geometrically corrected as remotely sensed data acquired by satellites represents the irregular surface of the earth. This was done by checking the satellite images against GoogleEarth and a vector Ordnance Survey (OS) MasterMap of Manchester downloaded from EDINA Digimap http://edina.ac.uk/digimap/. The GoogleEarth assessment shows that the Landsat and DMC image has an acceptable accuracy of 6.13m and 10.75m respectively. Subsets of satellite images were then generated to get the study area.

The Landsat image was stacked into a single layer as it has seven individual bands. The Landsat and DMC images were reprojected to Ordnance Survey Great Britain (OSGB). The study sites were then extracted from the full image using the subset image function. A 2km by 2km square perimeter was selected to bring out the details of the heavily urbanized area. All these processes were carried out in Erdas Imagine.

Image Classification

This is the process by which different classes or themes are extracted from raw remotely sensed digital satellite data [5,26,27]. Each pixel is usually considered to be a unique unit consisting of values in different spectral bands. By comparing pixels to one another and to pixels of known identity, users of remotely sensed data can assemble groups of identical pixels into classes [5,28].

Several classification methods have been proposed and developed for the derivation of land cover information from remotely sensed images. Unsupervised and supervised classification approach has been at the core of land cover mapping [29,30]. Unsupervised classification identifies structures or natural groups within a multispectral data, while supervised is the process by which samples of known identity are used to classify pixels of known identity.

The most widely used per-pixel approach, Maximum Likelihood Classification (MLC), was used in Erdas Imagine 2010. A land use land cover classification system like Anderson [18] was used for the classification. They are: (1) river (2) grassland (3) woodland (4) open space (5) motor way (6) railway (7) commercial buildings (8) residential buildings. It should be noted that the open class feature comprises of bare soils, construction sites and motor parks. These features were identified in the reference map and it was decided that they will be grouped into a single class called open space. This is to reduce errors in the classification process. Because training samples should represent the class to be identified, an aerial photograph was used to interpret different features of the images.

Classification Accuracy Assessment

Accuracy assessment is the comparison of two maps, one of which is based on the analysis of remotely sensed data and the other on a different source of information, usually a reference map that serves as the standard for comparison [31]. This is meant to express the classification's degree of 'correctness,' and it may be considered accurate if it can provide an unbiased representation of the region's land cover [32]. As a result, any disparity between the situation depicted on the thematic map and reality is referred to as a'classification error' [33]. Lillisand et al [34] states that; ‘a classification is not complete until its accuracy is assessed’. The most widely used and promoted is the error matrix which is also used in this research.

Error Matrix

Campbell [35] describes it as a simple cross-tabulation of the mapped class label against the observed in the ground or reference data for a sample of cases at specific locations”. It identifies overall errors for each category and identifies misclassifications by category [35]. Error matrix was used to establish the percentage of points allocated correctly to a feature class. Random sampling was used to establish data for the error matrix. This was accomplished by selecting random points on the aerial photograph and geo-linking the aerial photograph with the classified images in order to compare the same points directly. The random points on the aerial photographs are areas observed as river, grassland, woodland, motorway, railway, open space, commercial buildings and residential buildings. The feature class of the matched points were recorded in the error matrix section sharing the same feature class for both the aerial photograph and the classified image. The points that did not match were recorded in the column representing the feature class that the aerial photograph displayed and the classified image's class. A total of three hundred and twenty random points were used to compute the error matrix. The sum of the correctly classified pixels is then divided by the total number of random sample points.

Kappa Coefficient

To improve the overall accuracy assessment, Kappa coefficient is also employed. It is aimed at eliminating chance from the accuracy assessment process. The Kappa coefficient was calculated for the classified images using the Kappa coefficient equation culled from Foody [6].

$$\text{Kappa coefficient} = \frac{n\sum_{k=1}^{q} n_{kk} - \sum_{k=1}^{q} n_{k+}n_{+k}}{n^2 - \sum_{k=1}^{q} n_{k+}n_{+k}}$$

where

Predicted Class \ Actual Class	A	B	C	D	Σ
A	n_{AA}	n_{AB}	n_{AC}	n_{AD}	n_{A+}
B	n_{BA}	n_{BB}	n_{BC}	n_{BD}	n_{B+}
C	n_{CA}	n_{CB}	n_{CC}	n_{CD}	n_{C+}
D	n_{DA}	n_{DB}	n_{DC}	n_{DD}	n_{D+}
Σ	n_{+A}	n_{+B}	n_{+C}	n_{+D}	n

$$\text{Percentage correct} = \frac{\sum_{k=1}^{q} n_{kk}}{n} \times 100$$

$$\text{User's accuracy} = \frac{n_{ii}}{n_{i+}}$$

$$\text{Producer's accuracy} = \frac{n_{ii}}{n_{+i}}$$

Chi Square test

The Chi-square test was used to determine whether these results were statistically significant or if they happened by chance. It is a non-parametric test for categorical data analysis [36].

RESULTS

The essence of the analysis is to investigate how different sensors discriminate different land cover types. The results of these analyses will be presented in the subsections that follow. The resultant urban maps are also displayed to provide a visual land use pattern.

Unsupervised Classification

The colour infrared image result showed several correctly classified features, such as the river and buildings (Figure 3). However, the shadow of high-rise buildings has been classified as a river and the water fall on the River Irwell classified as a commercial building (figure 3).

There is little or no difference between the grassland and woodland feature classes as they are assigned to the same class (figure 3).

Some parts of the open space have been classified as commercial buildings (figure 3), and almost the whole residential buildings are classified as railway (figure 3). The motorway was correctly classified in some parts of the image.

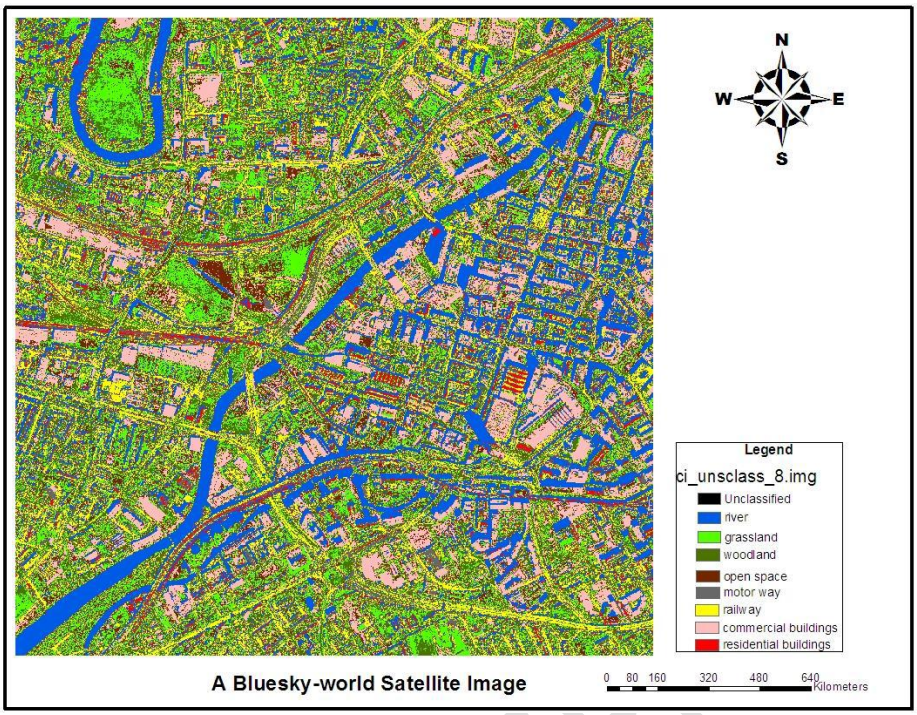

Figure 3: Unsupervised classification of the colour infrared satellite image.

DMC Satellite Image

This unsupervised classification is very pixelized (figure 4). Almost all the class features have been merged together. This is due to the DMC sensor's spatial resolution, which is 32m. This means a single pixel on the DMC image covers a ground area of 32m resulting in a greater percentage of the mixed pixel. The larger the percentage of mixed pixels, the more difficult it is to record and extract spatial detail in an image [37]. Linear features such as the railway and motor way cannot be easily identified.

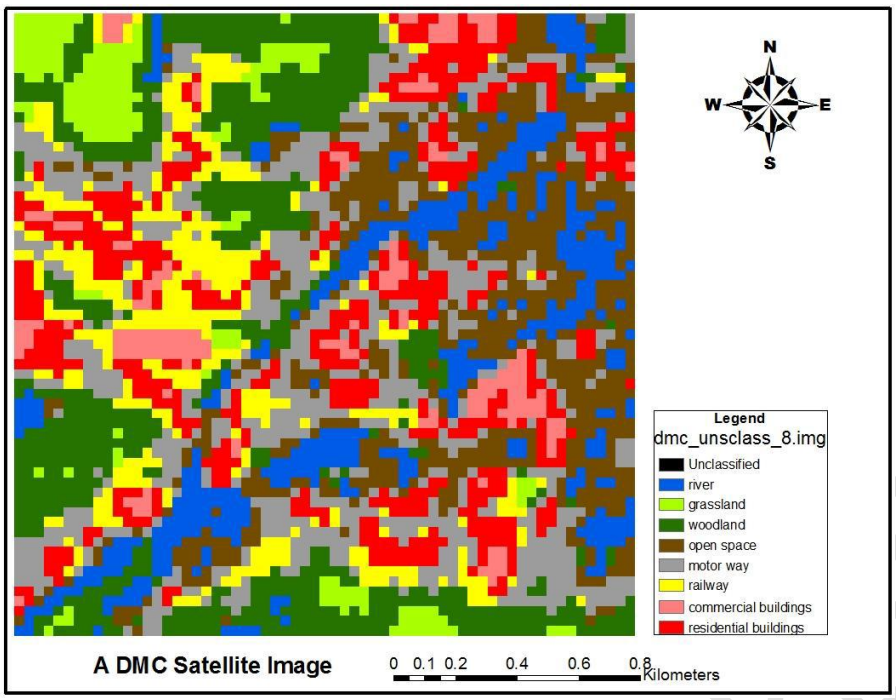

Figure 4: Unsupervised classification of the DMC Satellite Image

Most commercial buildings have also been classified as open space due to mixed pixels and because the spectral reflectance of the two features are similar. Features that have similar spectral reflectance to the river such as shadows of buildings have been classified as river.

The grassland and woodland along the Irwell River have been correctly identified. However, due to the sensor's spatial resolution, the woodland and river have been merged, resulting in mixed pixels. Along the edges of features, mixed pixels are common [38].

Landsat Satellite Image

Similarly, the unsupervised classification is also highly pixelized (figure 5). Because of their similar reflectance, most commercial buildings have been classified as residential and open spaces. Because the Landsat sensor has a spatial resolution of 30m, the pixels have been merged. This means that one Landsat pixel covers 30m of ground, resulting in mixed pixels. Similarly, linear features like railways and highways cannot be identified. The greater the percentage of mixed pixels in an image, the more difficult it is to record and extract spatial detail [38]. The grassland and woodland along the Irwell River have been correctly identified. The river and woodland, however, have been combined.

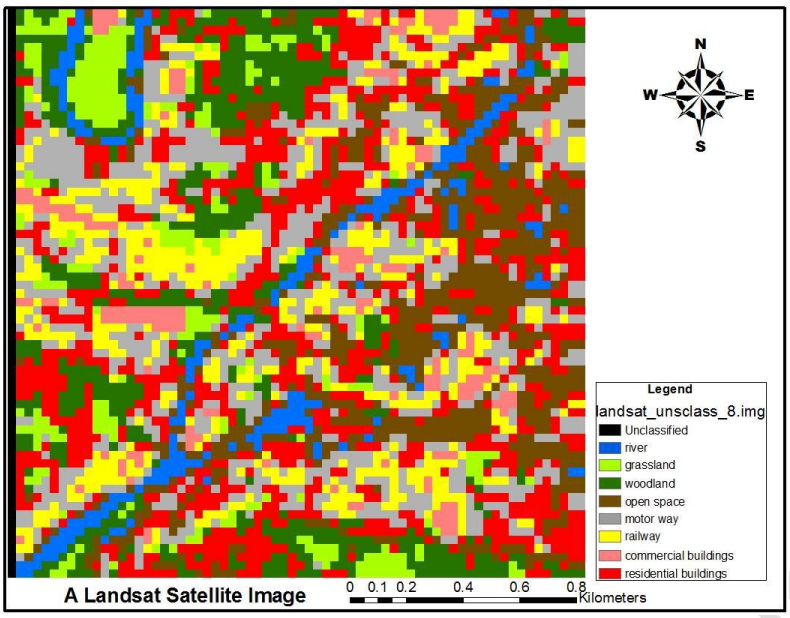

Figure 5: Unsupervised classification of the Landsat Satellite Image

Supervised Classification

The result of the unsupervised classification necessitated a supervised classification. Training areas on the image were identified and clearly matched to areas of known identity on the image which was used to run a supervised classification for the three satellite images.

Colour infrared Satellite Image

The supervised classification result shows that the building's shadows were correctly classified, not as a river, as in the unsupervised classification. However, the waterfall on the River Irwell is still classified as a commercial building due to its reflective properties. (figure 6). This means that the accuracy of correctly identifying landscape features was not absolute.

A careful selection of training areas yielded the correct classification of grassland and woodland (figure 6). Railway and motorways are also appropriately differentiated and correctly classified.

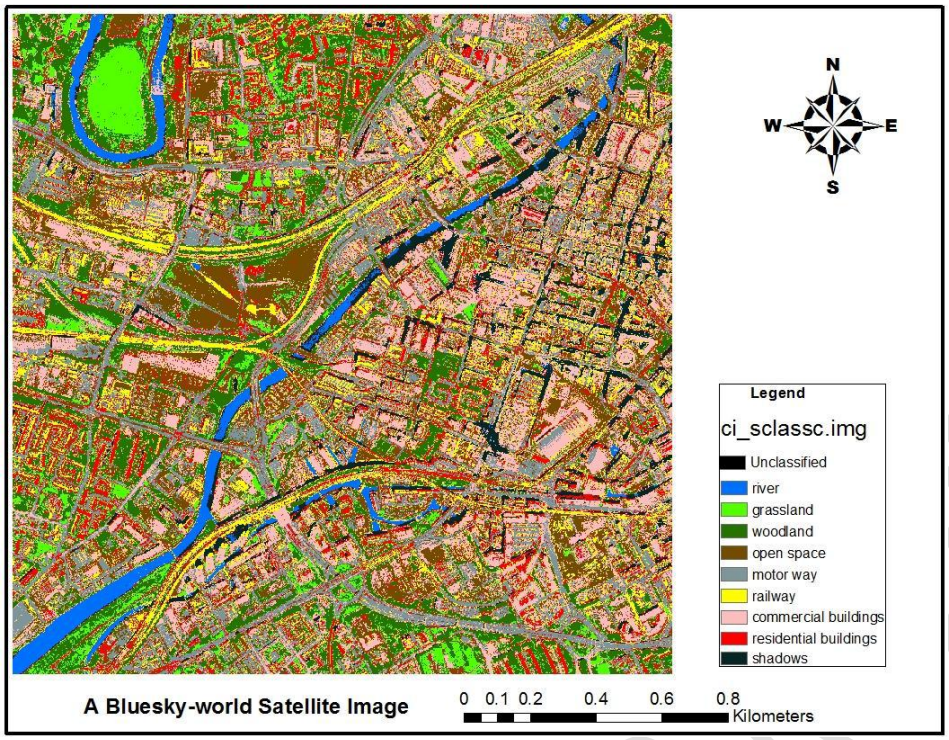

Figure 6: Supervised classification of the colour infrared satellite image.

Similarly, the residential and commercial properties have been classified correctly to a reasonable extent. The materials used in commercial buildings will be the same as those used in residential buildings, but the training area was carefully defined, as evidenced by the difference in the two-class feature in the color infrared image. However, some residential and commercial structures have been misclassified as railway and motorway..

Railway lines are typically made of steel or iron, buildings of a mix of clay, sand, wood, and rocks, and highways of sand, stone, and asphalt. Steel may be used in the construction of buildings or highways, depending on the nature of the construction, resulting in misclassification. Some sections of the railway line may also be built with stones. Furthermore, the spectral reflectance of these materials may be similar. Similarly, some open spaces have been mislabeled as roads. This is due to the fact that some of the open spaces are car parks that have been tarred with the same material as the motorway.

DMC Satellite Image

The result of the supervised classification shows a coarser image as compared to the colour infrared. (figure 7). The entire stretch of the river is not displayed with a high rate of mixed pixels. Similarly, the motorway and railway are not displayed linearly as they should. The commercial and residential buildings are more accurately classified here and have fewer mixed pixels unlike in the unsupervised classification. The woodland and grassland are not differentiated from one another due to mixed pixels. Similarly, the open space feature can barely

be seen. This is all due to the high spatial resolution of the sensor and mixed pixels which is common along the edges of features [38].

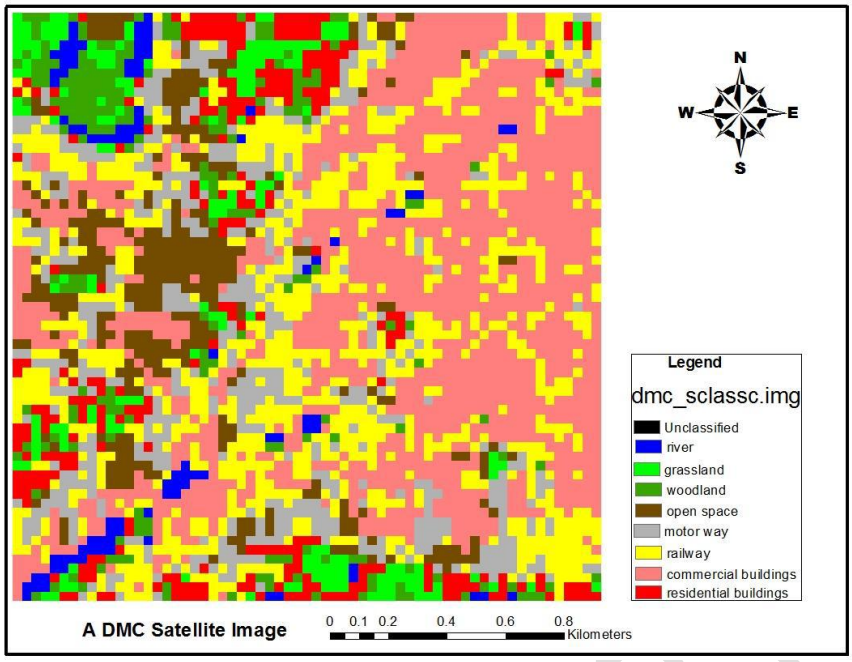

Figure 7: Supervised classification of the DMC Satellite Image.

Landsat Satellite Image

The result of the Landsat is similar to that of the DMC. The river is slightly more accurate as its linear feature can be seen (figure 8) however, there is also the occurrence of mixed pixels around it with grassland and woodland. The motor way and railway are not clearly depicted as linear features as the sensor`s resolution is not able to extract this information. Residential and commercial buildings are accurately displayed in their class feature however, there is still the occurrence of mixed pixels. Woodland and grassland are more accurately classified here than in the DMC. High level of mixed pixels exists in the open space. This is because 1m on the sensor covers 30m on the ground, therefore a lot of features have been merged.

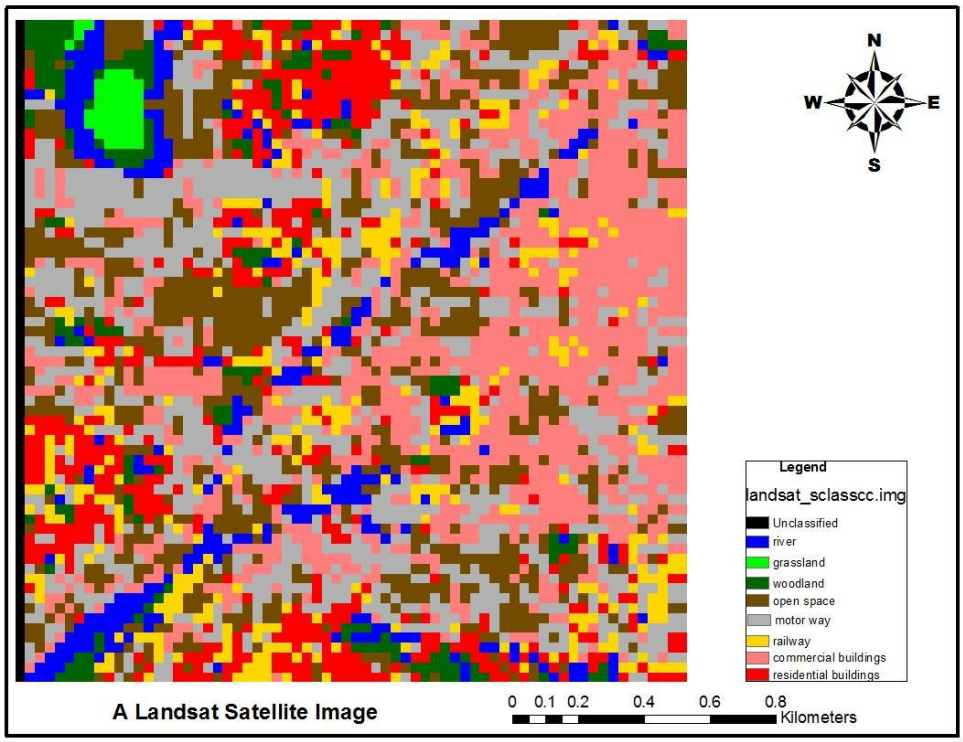

Figure 8: Supervised classification of the Landsat Satellite Image

Accuracy Assessment

Unsupervised Classification

The accuracy assessment of the unsupervised classified images shows that the colour infrared image has the highest accuracy of the pixels being correctly classified (table 1). This is followed by the Landsat (table 3) and then the DMC (table 2). The mixed pixels in the colour infrared can be attributed to the fact that some of the feature classes are made up of similar material and have the same spectral properties although they represent different classes on the map. For the DMC and Landsat, the spatial resolution of their sensors does not have the capability to map features in detail thereby resulting in mixed pixels.

Table 1: Colour Infrared Unsupervised Classification

	River	Grassland	Woodland	open space	Motor way	Railway	Commercial buildings	Residential buildings	Row total
River	**39**	0	0	0	0	0	1	0	40
Grassland	0	**30**	10	0	0	0	0	0	40
Woodland	0	23	**17**	0	0	0	0	0	40
Open space	0	0	0	**12**	10	0	18	0	40
Motor way	0	0	0	0	**34**	6	0	0	40
Railway	0	0	0	0	0	**33**	3	4	40
Commercial buildings	0	0	0	0	0	0	**38**	2	40
Residential buildings	0	0	0	0	0	30	0	**10**	40
Column total	39	53	27	12	44	69	59	17	320

Number of correctly classified pixels: 213

Total number of random points: 320

Correctly classified pixels: 67%

Kappa: 0.62

Table 2: DMC Unsupervised Classification

	River	Grassland	Woodland	open space	Motor way	Railway	Commercial buildings	Residential buildings	Row total
River	**15**	2	8	3	3	3	3	3	40
Grassland	0	**28**	5	4	0	0	0	3	40
Woodland	0	12	**15**	7	0	0	0	6	40
Open space	0	0	0	**10**	9	8	13	0	40
Motor way	0	0	0	9	**18**	7	6	0	40
Railway	0	4	0	10	10	**10**	4	2	40
Commercial buildings	0	0	0	10	5	0	**18**	7	40
Residential buildings	4	7	8	0	0	0	8	**13**	40
Column total	19	53	36	53	45	28	52	34	320

Number of correctly classified pixels: 127

Total number of random points: 320

Correctly classified pixels: 40%

Kappa: 0.31

Table 3: Landsat Unsupervised Classification

	River	Grassland	Woodland	open space	Motor way	Railway	Commercial buildings	Residential buildings	Row total
River	**20**	0	5	5	2	0	0	8	40
Grassland	0	**25**	5	5	0	0	0	5	40
Woodland	7	8	**18**	0	0	0	0	7	40
Open space	0	0	3	**21**	3	5	8	0	40
Motor way	4	0	0	10	**11**	7	0	8	40
Railway	0	0	2	7	6	**15**	5	5	40
Commercial buildings	0	0	0	3	0	4	**29**	4	40
Residential buildings	0	0	13	4	0	3	0	**20**	40
Column total	31	33	46	55	22	34	42	57	320

Number of correctly classified pixels: 159

Total number of random points: 320

Correctly classified pixels: 50%

Kappa: 0.43

Supervised Classification

The overall result is better than the unsupervised as training areas have been properly identified before the classification. The colour infrared image has the highest number of pixels correctly classified (table 4) However, the water fall on the river Irwell appeared as commercial buildings which was also the case for the unsupervised. Because the spectral property of the water fall is similar to that of commercial buildings, it has been incorrectly classified as such. Similarly, open space, railways, commercial and residential buildings have been classified incorrectly. The Landast has the next number of pixels correctly classified (table 6) followed by the DMC (table 5). The pixels are once again mixed due to the spatial resolution of their sensors.

Table 4: Colour infrared Supervised Classification

	River	Grassland	Woodland	open space	Motor way	Railway	Commercial buildings	Residential buildings	Row total
River	**39**	0	0	0	0	0	1	0	40
Grassland	0	**39**	1	0	0	0	0	0	40
Woodland	0	0	**40**	0	0	0	0	0	40
Open space	0	0	0	**20**	10	4	6	0	40
Motor way	0	0	0	0	**37**	0	0	3	40
Railway	0	0	0	0	0	**28**	7	5	40
Commercial buildings	0	0	0	5	4	3	**25**	3	40
Residential buildings	0	0	0	0	0	12	0	**28**	40
Column total	39	39	41	25	51	47	39	39	320

Number of correctly classified pixels: 256

Total number of random points: 320

Correctly classified pixels: 80%

Kappa: 0.77

Table 5: DMC Supervised Classification

	River	Grassland	Woodland	open space	Motor way	Railway	Commercial buildings	Residential buildings	Row total
River	**17**	3	4	2	2	3	5	4	40
Grassland	0	**20**	13	4	0	0	0	3	40
Woodland	0	10	**22**	3	0	0	0	5	40
Open space	0	0	0	**29**	4	3	4	0	40
Motor way	0	0	0	8	**17**	10	5	0	40
Railway	0	3	0	8	8	**12**	7	2	40
Commercial buildings	0	0	0	0	5	5	**30**	0	40
Residential buildings	0	3	3	3	3	3	0	**29**	40
Column total	17	39	42	57	39	36	51	43	320

Number of correctly classified pixels: 176

Total number of random points: 320

Correctly classified pixels: 55%

Kappa: 0.49

Table 6: Landsat Supervised Classification

	River	Grassland	Woodland	open space	Motor way	Railway	Commercial buildings	Residential buildings	Row total
River	**19**	5	4	4	0	4	4	0	40
Grassland	3	**27**	4	3	0	0	0	3	40
Woodland	3	0	**28**	3	0	0	3	3	40
Open space	0	0	3	**30**	0	0	7	0	40
Motor way	4	0	0	5	**22**	4	0	5	40
Railway	0	0	4	5	6	**18**	4	3	40
Commercial buildings	0	0	0	6	0	5	**25**	4	40
Residential buildings	2	0	4	5	0	4	0	**25**	40
Column total	31	32	47	61	28	35	43	43	320

Number of correctly classified pixels: 194

Total number of random points: 320

Correctly classified pixels: 61%

Kappa: 0.55

Chi-Square test

Using our degree of freedom which is 7, the unsupervised coloured infrared with a chi square of 60.075(table 7) has a p-value of $p < 0.001$. The unsupervised DMC with a chi-square value of 122.275 has a p-value of $p < 0.001$ while the Landsat with a chi-square of 86.425 has a p-value of $p < 0.001$. Since the three images have a p value of $p < 0.001$, using 0.05 as our significant level, we reject the null hypothesis which states that there is no significant relationship between the classified images and their sensors. That is the sensors have differential capability to discriminate among ground features.

For the supervised colour infrared image with a chi square value of 23.1, (table 8) the p-value is 0.00163. The supervised DMC image with a chi square value of 72.7 has a p-value of $p < 0.001$ while the supervised Landsat image with a chi square value of 52.8 and a p-value of $p < 0.001$. They are all less than our significant level of 0.05. Therefore, we reject the null hypothesis which states that there is no significant relationship between the classified images and their sensor. This means the sensors have differential capabilities to discriminate among ground features.

Table 7: Unsupervised Classification Chi Square Test

Urban Land use type	Colour Infrared		DMC		Landsat TM	
	Observed-Expected	$(O-E)^2/E$	O-E	$(O-E)^2/E$	O-E	$(O-E)^2/E$
River	39 - 40	0.025	15 - 40	15.625	20 - 40	10
Grassland	30 - 40	2.5	28 - 40	3.6	25 - 40	5.625
Woodland	17 - 40	13.225	15 - 40	15.625	18 - 40	12.1
Open space	12 - 40	19.6	10 - 40	22.5	21 - 40	9.025
Motor way	34 - 40	0.9	18 - 40	12.1	11 - 40	21.025
Railway	33 - 40	1.225	10 - 40	22.5	15 - 40	15.625
Commercial buildings	38 - 40	0.1	18 - 40	12.1	29 - 40	3.025
Residential buildings	10 - 40	22.5	13 - 40	18.225	20 - 40	10
Chi-Square (Total)		**60.075**		**122.275**		**86.425**

Table 8: Supervised Classification Chi-Square Test

Urban Land use type	Colour Infrared		DMC		Landsat TM	
	Observed-Expected	$(O-E)^2/E$	O-E	$(O-E)^2/E$	O-E	$(O-E)^2/E$
River	39 - 40	0.025	17 - 40	13.225	19 - 40	11.025
Grassland	39 - 40	0.025	20 - 40	10	27 - 40	4.225
Woodland	40 - 40	0	22 - 40	8.1	28 - 40	3.6
Open space	20 - 40	10	29 - 40	3.025	30 - 40	2.5
Motor way	37 - 40	0.225	17 - 40	13.225	22 - 40	8.1
Railway	28 - 40	3.6	12 - 40	19.6	18 - 40	12.1
Commercial buildings	25 - 40	5.625	30 - 40	2.5	25 - 40	5.625
Residential buildings	28 - 40	3.6	29 - 40	3.025	25 - 40	5.625

Chi-Square (Total)		**23.1**		**72.7**		**52.8**

DISCUSSION

The unsupervised classification aided understanding the land cover structure and identification of homogenous clusters in the satellite image. The shadow of the high rise building was classified as a river and the water fall on the River Irwell classified as a commercial building because unsupervised classification can only identify spectrally homogenous classes within the data that may not in fact correspond to the informational categories [33,39]. Within multispectral data, it also identifies natural groups as remotely sensed images are made up of classes that are uniform internally with respect to brightness in several spectral channels. In the light of this, the building shadows have the same reflection with the river which made it automatically pick and identify it as part of the river. Rivers may appear dark or light in tone depending on the time of the day they were imaged. Similarly, the waterfall on the river and the commercial buildings have the same reflectance. River Irwell has an entrenched channel and this may prevent reflected electromagnetic radiation (EMR) from reaching the sensor, so the river appears dark.

The grassland and woodland were merged into one class because living vegetation appears as bright red in false colour composite. Thapa and Murayama [40] obtained similar low accuracy result and they discovered that unsupervised classification usually fails or overestimate the heterogeneity of landscapes, particularly in residential and suburban areas. The complexity of urban environment may be responsible for this as it compels the classifier to overestimate land use and land cover area. Both grassland and woodland are green, hence their spectral signature is similar.

The result of the supervised classification yielded better accuracy than the unsupervised. For the colour infrared image which has a spatial resolution of 0.125m, its accuracy improved from 67% (unsupervised) to 80% (supervised). Even after matching spectrally homogeneous classes, open space, motorway, railway, and commercial and residential buildings were still misclassified. Some of the residential and commercial houses were misclassified as railway and motorway. Railway lines are generally made from steel. Aluminum and steel are two other popular roofing materials. In some areas of the railway line, stones may also be used . Also, these materials may have similar spectral reflectance. Some open spaces were misclassified as motor way. This is because some of the open spaces are car parks which are tarred with similar materials used for the motor way. The underlying factor of this is “spectral resolution”. Price [41] believes that such spectral variability in the dataset results from urban or man-made features. He further suggested that more or different bands would be required to assess these surface types spectrally. Herold [42] discovered that even after using twenty-six different urban land cover classes and hyperspectral optical remote sensing data, certain land cover types still have similar spectral characteristics.

Researchers have attempted to fuse multi-source remote sensing data with medium-resolution images. This improves the overall resolution, increases model accuracy, and makes change detection more noticeable [6]. Jia et al.[15] fused Landsat 8 Operating Land Imager (OLI) NDVI at 30m with MODIS NDVI at 250m. This method was proposed to improve land cover classification and it yielded a 4 per cent improvement in the overall classification accuracy compared to a single temporal Landsat data. Singh et al [43] demonstrated that the combination of LiDAR and Landsat data can lead to increased accuracy in discriminating heterogenous land cover over large urban regions.

Xia et al.[16] combined multi-source features from remote sensing data and geolocation datasets to extract information on large-scale urban areas using random forest classifier. The classification results were in good accordance with the urban boundaries however, the model revealed an obvious misclassification of the river and lake regions due to coarse resolution.

The major finding here is that both supervised and unsupervised classification of remotely sensed images could not differentiate between car parks, roads, and buildings as their spectral signatures are the same due to similar construction materials. This can be attributed to the fact that land use type does not typically hold unique physical characteristics [44]. This emphasizes the need for ground truthing when using satellite images for urban land cover analysis especially when low resolution satellites are used at micro level. Therefore, ground truthing is very crucial and should be embarked upon for accurate verification of land cover. Xia et al [16] proposed a systematic evaluation of the reliability of web-sourced GIS data. This can be achieved by applying more remote sensing and GIS data to extract urban areas at a large scale particularly datasets with a finer spatial resolution. There has been an advancement in the capabilities of cloud-based computational platforms [44]. It allows analysis of land use land cover characteristics of the earth across a greater geographical and temporal scale. While land cover refers to the attributes of the earth land surface and its immediate subsurface, land use refers to the purpose for which humans exploit the land cover [45]. Remote sensing observations typically capture the unique reflectance characteristics of physical objects on earth, which makes most remote sensing applications focus on detecting and classifying the land cover characteristics of earth [44]. However, differentiating between different land use types remains challenging [44].

Very good spatial resolution images like the color infrared usually come at a very high cost and do not usually cover a large area, unlike the Landsat and DMC, which can cover an entire state or city and are usually free of charge.

The statistical tests for the images also prove that the accuracy of urban land cover mapping is highly dependent on the spatial resolution of the sensor. The Chi Square test revealed that there is a strong relationship between the classified images and their sensors. The higher the spatial resolution of the sensor, the more detailed information can be derived from the satellite images and the better the accuracy assessment.

CONCLUSION

Remote sensing of urban areas can be a difficult task as the remotely sensed data can only pick land cover types and land cover use. The researcher can specify the number of categories or classes in supervised classification. However, matching spectral classes is usually a problem as it only identifies spectrally homogenous classes within the data. It may be sometimes necessary to have several classes so that spectrally homogenous classes can further be separated into more classes. However, this can only be very effective if the spatial resolution of the sensors is good enough to map out urban details. The unsupervised classification aided in understanding the land cover structure and identifying homogenous clusters in the imagery.

The colour infrared image is the most suitable for urban land cover analysis as the misclassifications are minimal compared to the other two and the features can be vividly recognized due to its spatial resolution.

REFERENCES

[1] Thakur JK, Singh SK, Ekanthalu VS. Integrating remote sensing, geographic information systems and global positioning system techniques with hydrological modeling. Appl Water Sci 2017;7:1595–608. https://doi.org/10.1007/s13201-016-0384-5.

[2] Zhou X, Ding Y, Wu C, Huang J, Hu C. Measuring the spatial allocation rationality of service facilities of residential areas based on internet map and location-based service data. Sustain 2019;11:1–20. https://doi.org/10.3390/su11051337.

[3] Lv Q, Dou Y, Niu X, Xu J, Xu J, Xia F. Urban land use and land cover classification using remotely sensed sar data through deep belief networks. J Sensors 2015;2015:1–11. https://doi.org/10.1155/2015/538063.

[4] Gómez C, White JC, Wulder MA. Optical remotely sensed time series data for land cover classification: A review. ISPRS J Photogramm Remote Sens 2016;116:55–72. https://doi.org/10.1016/j.isprsjprs.2016.03.008.

[5] Qin R, Liu T. A Review of Landcover Classification with Very-High Resolution Remotely Sensed Optical Images—Analysis Unit, Model Scalability and Transferability. Remote Sens 2022;14:1–28. https://doi.org/10.3390/rs14030646.

[6] Kadhim N, Mourshed M, Bray M. Advances in remote sensing applications for urban sustainability. Euro-Mediterranean J Environ Integr 2016;1:1–22. https://doi.org/10.1007/s41207-016-0007-4.

[7] El Garouani A, Mulla DJ, El Garouani S, Knight J. Analysis of urban growth and sprawl from remote sensing data: Case of Fez, Morocco. Int J Sustain Built Environ 2017;6:160–9. https://doi.org/10.1016/j.ijsbe.2017.02.003.

[8] Agapiou A. Optimal spatial resolution for the detection and discrimination of archaeological proxies in areas with spectral heterogeneity. Remote Sens 2020;12:1–21. https://doi.org/10.3390/RS12010136.

[9] Sertel E, Akay SS. High resolution mapping of urban areas using SPOT-5 images and ancillary data. Int J Environ Geoinformatics 2015;2:63–76.

https://doi.org/10.30897/ijegeo.303545.

[10] Vanjare A, Omkar SN, Senthilnath J. Satellite Image Processing for Land Use and Land Cover Mapping. Int J Image, Graph Signal Process 2014;6:18–28. https://doi.org/10.5815/ijigsp.2014.10.03.

[11] Fisher JRB, Acosta EA, Dennedy-Frank PJ, Kroeger T, Boucher TM. Impact of satellite imagery spatial resolution on land use classification accuracy and modeled water quality. Remote Sens Ecol Conserv 2018;4:137–49. https://doi.org/10.1002/rse2.61.

[12] Ahmed S. Comparison of Satellite Images Classification Techniques using Landsat-8 Data for Land Cover Extraction. Int J Intell Comput Inf Sci 2021;0:1–15. https://doi.org/10.21608/ijicis.2021.78853.1098.

[13] Li M, Zang S, Zhang B, Li S, Wu C. A review of remote sensing image classification techniques: The role of Spatio-contextual information. Eur J Remote Sens 2014;47:389–411. https://doi.org/10.5721/EuJRS20144723.

[14] Zhou T, Li Z, Pan J. Multi-feature classification of multi-sensor satellite imagery based on dual-polarimetric sentinel-1A, landsat-8 OLI, and hyperion images for urban land-cover classification. Sensors (Switzerland) 2018;18:1–20. https://doi.org/10.3390/s18020373.

[15] Jia K, Liang S, Zhang N, Wei X, Gu X, Zhao X, et al. Land cover classification of finer resolution remote sensing data integrating temporal features from time series coarser resolution data. ISPRS J Photogramm Remote Sens 2014;93:49–55. https://doi.org/10.1016/j.isprsjprs.2014.04.004.

[16] Xia N, Cheng L, Li MC. Mapping urban areas using a combination of remote sensing and geolocation data. Remote Sens 2019;11:1–23. https://doi.org/10.3390/rs11121470.

[17] Islami FA, Tarigan SD, Wahjunie ED, Dasanto BD. Accuracy Assessment of Land Use Change Analysis Using Google Earth in Sadar Watershed Mojokerto Regency. IOP Conf Ser Earth Environ Sci 2022;950:1–9. https://doi.org/10.1088/1755-1315/950/1/012091.

[18] Anderson JR, Hardy EE, Roach JT, Witmer RE. Land Use and Land Cover Classification System for Use With Remote Sensor Data. U S Geol Surv, Prof Pap 1976:1–34.

[19] NASA. The Landsat 7 compositor: How are satellite images different from photographs? Natl Aeronaut Sp Adm 2011:1–10. https://www.colby.edu/biology/BI352/Labs/satelliteim_info.pdf (accessed May 12, 2022).

[20] Steven MD. Ground truth an underview. Int J Remote Sens 1987;8:1033–8.

https://doi.org/10.1080/01431168708954745.

[21] Chen F, Zhao X, Ye H. Making Use of the Landsat 7 SLC-off ETM+ Image Through Different Recovering Approaches. Data Acquis. Appl., 2012. https://doi.org/10.5772/48535.

[22] Bayr U. Quantifying historical landscape change with repeat photography: an accuracy assessment of geospatial data obtained through monoplotting. Int J Geogr Inf Sci 2021;35:2026–46. https://doi.org/10.1080/13658816.2021.1871910.

[23] Anurogo W, Lubis MZ, Khoirunnisa H, Pamungkas DS, Hanafi A, Rizki F, et al. A Simple Aerial Photogrammetric Mapping System Overview and Image Acquisition Using Unmanned Aerial Vehicles (UAVs). J Appl Geospatial Inf 2017;1:11–8. https://doi.org/10.30871/jagi.v1i01.360.

[24] Korsgaard NJ, Nuth C, Khan SA, Kjeldsen KK, Bjørk AA, Schomacker A, et al. Digital elevation model and orthophotographs of Greenland based on aerial photographs from 1978-1987. Sci Data 2016;3:1–15. https://doi.org/10.1038/sdata.2016.32.

[25] Siok K, Ewiak I. The simulation approach to the interpretation of archival aerial photographs. Open Geosci 2020;12:1–10. https://doi.org/10.1515/geo-2020-0001.

[26] Khorram S, Nelson SAC, van der Wiele CF, Cakir H. Processing and Applications of Remotely Sensed Data. Handb. Satell. Appl., 2017, p. 1017–46. https://doi.org/10.1007/978-3-319-23386-4_92.

[27] Asokan A, Anitha J, Ciobanu M, Gabor A, Naaji A, Hemanth DJ. Image processing techniques for analysis of satellite images for historical maps classification-An overview. Appl Sci 2020;10:1–21. https://doi.org/10.3390/app10124207.

[28] Goswami A, Sharma D, Mathuku H, Gangadharan SMP, Yadav CS, Sahu SK, et al. Change Detection in Remote Sensing Image Data Comparing Algebraic and Machine Learning Methods. Electron 2022;11:1–26. https://doi.org/10.3390/electronics11030431.

[29] Ma Z, Liu Z, Zhao Y, Zhang L, Liu D, Ren T, et al. An unsupervised crop classification method based on principal components isometric binning. ISPRS Int J Geo-Information 2020;9:1–24. https://doi.org/10.3390/ijgi9110648.

[30] Comer PJ, Hak JC, Dockter D, Smith J. Integration of vegetation classification with land cover mapping: lessons from regional mapping efforts in the Americas. Veg Classif Surv 2022;3:29–43. https://doi.org/10.3897/vcs.67537.

[31] Pisharoty PR. Introduction to remote sensing. Proc Indian Acad Sci Sect C Eng Sci 1983;6:97–107. https://doi.org/10.1007/BF02842927.

[32] Aune-Lundberg L, Strand GH. The content and accuracy of the CORINE Land Cover dataset for Norway. Int J Appl Earth Obs Geoinf 2021;96:1–10. https://doi.org/10.1016/j.jag.2020.102266.

[33] Radoux J, Bogaert P. Good practices for object-based accuracy assessment. Remote Sens 2017;9:1–23. https://doi.org/10.3390/rs9070646.

[34] Lillesand TM, Kiefer RW. Remote sensing and image interpretation. 1979. https://doi.org/10.2307/634969.

[35] Cracknell AP, Hayes LBW. Introduction to remote sensing. 1991. https://doi.org/10.1117/3.673407.ch1.

[36] Singhal R, Rana R. Chi-square test and its application in hypothesis testing. J Pract Cardiovasc Sci 2015;1:69–71. https://doi.org/10.4103/2395-5414.157577.

[37] Ma L, Li M, Ma X, Cheng L, Du P, Liu Y. A review of supervised object-based land-cover image classification. ISPRS J Photogramm Remote Sens 2017;130:277–93. https://doi.org/10.1016/j.isprsjprs.2017.06.001.

[38] Choodarathnakara AL, Kumar TA, Koliwad S, Patil CG. Mixed Pixels: A Challenge in Remote Sensing Data Classification for Improving Performance. Int J Adv Res Comput Eng Technol 2012;1:261–71.

[39] Pretorius E, Pretorius R. Improving the potential of pixel-based supervised classification in the absence of quality ground truth data. South African J Geomatics 2015;4:250–64. https://doi.org/10.4314/sajg.v4i3.6.

[40] Thapa RB, Murayama Y. Examining spatiotemporal urbanization patterns in Kathmandu Valley, Nepal: Remote sensing and spatial metrics approaches. Remote Sens 2009;1:534–56. https://doi.org/10.3390/rs1030534.

[41] Price JC. Spectral band selection for visible-near infrared remote sensing: Spectral-spatial resolution tradeoffs. IEEE Trans Geosci Remote Sens 1997;35:1277–85. https://doi.org/10.1109/36.628794.

[42] Herold M, Gardner ME, Roberts DA. Spectral resolution requirements for mapping urban areas. IEEE Trans Geosci Remote Sens 2003;41:1907–19. https://doi.org/10.1109/TGRS.2003.815238.

[43] Singh KK, Vogler JB, Shoemaker DA, Meentemeyer RK. LiDAR-Landsat data fusion for large-area assessment of urban land cover: Balancing spatial resolution, data volume and mapping accuracy. ISPRS J Photogramm Remote Sens 2012;74:110–21. https://doi.org/10.1016/j.isprsjprs.2012.09.009.

[44] Goldblatt R, Jones N, Mannix J. assessing OpenStreetMap completeness for management of natural disaster by means of remote sensing: A case study of three small Island States (Haiti, Dominica and St. Lucia). Remote Sens 2020;12:1–25. https://doi.org/10.3390/RS12010118.

[45] Nedd R, Light K, Owens M, James N, Johnson E, Anandhi A. A synthesis of land use/land cover studies: Definitions, classification systems, meta-studies, challenges and knowledge gaps on a global landscape. Land 2021;10:1–30. https://doi.org/10.3390/land10090994.